COVER SHEET

The molecular structure of selected minerals of the rosasite group - an XRD, SEM and infrared spectroscopic study

Ray L. Frost•, Daria L. Wain, Wayde N. Martens and B. Jagannadha Reddy

Inorganic Materials Research Program, School of Physical and Chemical Sciences, Queensland University of Technology, GPO Box 2434, Brisbane Queensland 4001, Australia.

Abstract

Minerals of the rosasite group namely, rosasite, glaucosphaerite, kolwezite, mcguinnessite have been studied by powder X-ray diffraction, scanning electron microscopy and infrared spectroscopy. X-ray diffraction shows the minerals to be complex mixtures with more than one rosasite mineral observed in each sample. SEM analysis shows the minerals to be fibrous in nature and the use of EDAX enabled the chemical composition of the minerals to be determined. The spectral patterns for the rosasite minerals are similar to that of malachite implying the molecular structure of is similar. The rosasite minerals are characterised by two OH stretching vibrations at ~3401 and 3311 cm^{-1}. Two intense bands observed at ~ 1096 and 1046 cm^{-1} are assigned to ν_1 $(CO_3)^{2-}$ symmetric stretching vibration and the δ OH deformation mode. Multiple bands are found in the 800 to 900 cm^{-1} and 650 to 750 cm^{-1} regions attributed to the ν_2 and ν_4 bending modes confirming the symmetry reduction of the carbonate anion in rosasites as C_{2v} or C_s. A band at ~560 cm^{-1} is assigned to a CuO stretching mode.

Key words: glaucosphaerite, kolwezite, mcguinnessite, nullaginite, rosasite, hydroxycarbonate, Infrared spectroscopy

Introduction

The carbonates are a group of over 60 naturally occurring minerals containing the essential structural building block $(CO_3)^{2-}$. Most of these minerals are relatively rare and often in association with other building blocks such as hydroxyls, halogens, sulphate, silicate, phosphate, etc. The common simple rock-forming carbonates can be divided into three main groups: a) the calcite group, b) the dolomite group and c) the aragonite group. Peter Williams reports that whilst metal substitution in azurite is extremely uncommon, such is not the case for malachite [1]. Substitution of Cu(II) by other cations gives rise to the rosasite mineral group. In minerals related to malachite, ions identified together with Cu(II) are: Zn(II), Co(II), Ni(II) and Mg(II). The rosasite mineral group is monoclinic or triclinic hydroxy carbonates with the general formula $A_2(CO_3)(OH)_2$ or $AB(CO_3)(OH)_2$ where A and B is cobalt, copper, magnesium, nickel and zinc [2]. The most common congener of malachite is rosasite. Rosasite forms in the oxidation zones of zinc-copper deposits and the crystals are often fibrous and found in tufted aggregates. No single crystal study of rosasite has been forth coming. Powder diffraction studies of rosasite suggest the mineral is triclinic [3]. The chemical composition of the rosasite minerals means that the minerals are highly

• Author to whom correspondence should be addressed (r.frost@qut.edu.au)

colourful, often green to blue. Minerals in the rosasite group are related to the mineral malachite [4, 5]. Minerals in this group include rosasite [$(Cu,Zn)_2(CO_3)(OH)_2$] [6-8], glaucosphaerite [$(Cu,Ni)_2(CO_3)(OH)_2$] [9-11], kolwezite [$(Cu,Co)_2(CO_3)(OH)_2$] [12], mcguinnessite [$(Mg,Cu,)_2(CO_3)(OH)_2$] [13-16], and nullaginite [$(Ni)_2(CO_3)(OH)_2$] [17-19]. Apart from rosasite the minerals are rare secondary minerals. Besides the chemical composition, the structural relationships between these minerals are demonstrated by the similarity of their powder diffraction patterns [20]. The space group symmetry and cell parameters are mainly derived from powder pattern indexing. Apart from that of malachite, no other structural determinations are available for the rosasite minerals. Rosasite as with the other minerals of this group form spheroidal aggregates in extremely thin fibrous crystals. Rosasite may be associated with aurichalcite, smithsonite and hemimorphite.

Infrared and Raman spectroscopy have been used to investigate carbonates including azurite and malachite [21, 22]. A detailed single crystal Raman study has been undertaken [5, 21]. However the vibrational spectroscopy of minerals of the rosasite group has not been undertaken. No infrared spectra of the minerals of the rosasite group have been forthcoming [22-25]. Also no NIR research on these minerals has been reported. An infrared stretching vibration of the hydroxyl unit of azurite was observed at 3425 cm^{-1}, whereas two bands were reported for malachite at 3400 and 3320 cm^{-1}. The observation of two bands for malachite suggests coupling of the hydroxyl stretching vibrations [5]. This coupling was not observed for azurite [5]. Azurite and malachite form the basis of pigments in samples of an archaeological or medieval nature [26-29]. Malachite has a characteristic intense band at ~430 cm^{-1} and for azurite an intense band at ~400 cm^{-1}. The deformation modes of azurite were reported at 1035 and 952 cm^{-1} and at 1045 and 875 cm^{-1} for malachite. [22, 30] Thus even though the two carbonate minerals have the same space group, the molecular structure of the minerals is sufficiently different to show infrared bands at slightly different wavenumbers. Differences between the spectra of malachite and azurite may be explained by the molecular structure of azurite being based upon a distorted square planar arrangement compared with a distorted octahedral arrangement about the copper in malachite.

The symmetric stretching bands of carbonate for azurite and malachite were observed at 1090 and 1095 cm^{-1}. Goldsmith and Ross reported the infrared bending modes of carbonate at 837 and 817 cm^{-1} for azurite and at 820 and 803 cm^{-1} for malachite [21]. Two ν_3 modes were observed at 1490 and 1415 cm^{-1} for azurite and at 1500 and 1400 cm^{-1} for malachite [4, 5]. The observation of these two bands shows a loss of degeneracy. Such a conclusion is also supported by the observation of two ν_4 modes at 769 and 747 cm^{-1} for azurite and 710 and 748 cm^{-1} for malachite. The vibrational spectroscopy of these two minerals is complicated by this loss of degeneracy. Schmidt and Lutz report some vibrational spectroscopic data [31]. Two infrared bands at 3415 and 3327 cm^{-1} were observed for malachite. Although the Raman spectra of the mineral brochantite [$Cu_4(OH)_6SO_4$] have been reported, the Raman spectra of malachite and azurite were not [31].

In this work we report the X-ray diffraction, SEM analysis and infrared spectroscopy of minerals of the rosasite group and relate the spectroscopy to the mineral structure.

Experimental

Minerals

The minerals, their formula and origin used in this study are listed in Table 1. Selected minerals were obtained from the Mineral Research Company and other sources including Museum Victoria. The samples were phase analysed by X-ray diffraction for phase analysis and for chemical composition by EDX measurements.

X-Ray diffraction

X-ray diffraction (XRD) patterns were recorded using CuKα radiation (n = 1.5418Å) on a Philips PANalytical X' Pert PRO diffractometer operating at 40 kV and 40 mA with 0.125° divergence slit, 0.25° anti-scatter slit, between 3 and 15° (2θ) at a step size of 0.0167°. For low angle XRD, patterns were recorded between 1 and 5° (2θ) at a step size of 0.0167° with variable divergence slit and 0.5° anti-scatter slit.

SEM Analysis

Mineral samples of the rosasite were coated with a thin layer of evaporated carbon and secondary electron images were obtained using an FEI Quanta 200 scanning electron microscope (SEM). For X-ray microanalysis (EDX), three samples were embedded in Araldite resin and polished with diamond paste on Lamplan 450 polishing cloth using water as a lubricant. The samples were coated with a thin layer of evaporated carbon for conduction and examined in a JEOL 840A analytical SEM at 25kV accelerating voltage. Preliminary analyses of the rosasite mineral samples were carried out on the FEI Quanta SEM using an EDAX microanalyser, and microanalysis of the clusters of fine crystals was carried out using a full standards quantitative procedure on the JEOL 840 SEM using a Moran Scientific microanalysis system. Oxygen was not measured directly but was calculated using assumed stoichiometries to the other elements analysed.

Mid-IR spectroscopy

Infrared spectra were obtained using a Nicolet Nexus 870 FTIR spectrometer with a smart endurance single bounce diamond ATR cell. Spectra over the 4000–525 cm^{-1} range were obtained by the co-addition of 64 scans with a resolution of 4 cm^{-1} and a mirror velocity of 0.6329 cm/s. Spectra were co-added to improve the signal to noise ratio.

Spectral manipulation such as baseline adjustment, smoothing and normalisation were performed using the Spectracalc software package GRAMS (Galactic Industries Corporation, NH, USA). Band component analysis was undertaken using the Jandel 'Peakfit' software package which enabled the type of fitting function to be selected and allows specific parameters to be fixed or varied accordingly. Band fitting was done using a Lorentz-Gauss cross-product function with the minimum number of component bands used for the fitting process. The Gauss-Lorentz ratio was

maintained at values greater than 0.7 and fitting was undertaken until reproducible results were obtained with squared correlations of r^2 greater than 0.995.

Results and discussion

X-ray diffraction

The XRD patterns of the rosasite mineral group are illustrated by those of rosasite and glakosphaerite which are shown in Figures 1a and 1b. What is observed from the XRD patterns is that the mineral rosasite appears to be a mixture of rosasite, quartz and mcguinnessite. Glaukosphaerite appears to be a mixture of glaukosphaerite with some malachite and other impurities. In order to run an XRD pattern the mineral is scraped off a host rock and is ground before the XRD pattern is collected. This means that all minerals present are analysed. In terms of SEM and spectroscopy a more judicious selection can be made and only specific crystals analysed. In this instance the correct mineral is obtained. Roberts et al. showed that the mineral rosasite was monoclinic [32].

SEM images

SEM images of rosasite, glaucosphaerite, kolwezite and pokrovskite are shown in Figures 2a, 2b, 2c and 2d. The crystals of the three minerals are acicular and may be up to 0.5 mm in length. The minerals appear to be fibrous in nature. The images show the hydroxycarbonates to be botryoidal and forming crusts. This is best illustrated by the SEM image of pokrovskite (Figure 2d). Figures 3 show the typical EDAX analyses of rosasite, gluakosphaerite, kolwezite and mcguinessite. The results of the analyses are reported in Table 1.

The rosasite sample used in this work analysed to a Cu/Zn ratio of close to 1:1. As such if the atom ratio of Cu/Zn is 1:1 then every second position in the model will be taken up by a Zn atom. Rosasite does not necessarily maintain a ratio of 1:1. For example the rosasite from Rosas mine, Narcao, Cagliari, Sardegna (Sardinia), Italy analyses as CuO 53.7 and ZnO 18.3 %. This gives a formula of the Narcao rosasite as $(Cu_{1.5}Zn_{0.5})_2(CO)_3(OH)_2$. According to Anthony et al. a glaucosphaerite sample from Kasompi, Congo gave a formula of $(Cu_{1.23}Zn_{0.71})_2(CO)_3(OH)_2$ [33]. It is noted that the Cu/Zn ratio is not 1:1 and the total cations is not 2.0, but 1.94. The mineral glaucosphaerite from the Carr Boyd Nickel mine analyses as CuO 41.6 % and NiO 25.2 %. This gives the formula of glaucosphaerite as $(Cu_{1.1}Ni_{0.7}Mg_{0.06})_2(CO)_3(OH)_2$. A similar formula exists for the mineral kolwezite from Zaire namely $(Cu_{1.33}Co_{0.67})_2(CO)_3(OH)_2$. The fact that the two cation ratio is not 1:1 may have implications for the structure of the mineral and therefore for the vibrational spectroscopy of the mineral. The mcguinnessite from California gives a cation ratio of Cu/Mg as 1:1. Other measurements record a ratio of Mg/Cu as 1.5/0.5.

Infrared spectroscopy

The minerals of the rosasite group have not been studied by single crystal X-ray diffraction. Invariably because most of the crystals are composed of thin fibres.

Extensive powder X-ray diffraction suggests the minerals are triclinic, although Anthony et el. states the minerals are monoclinic [33]. This statement is apparently based upon the assumption the structures are similar to that of malachite. The structure shows that two of the three oxygens bond to separate copper atoms but one carbonate oxygen bonds to two copper atoms. The OH unit serves to bridge two copper atoms. The model of the structure of malachite shows that the carbonate anion is of C_{2v} symmetry if the two cations bonding to the carbonate anion are identical [4, 5]. If however the two cations are different (e.g. Cu and Ni or Cu and Zn) then the symmetry of the carbonate anion would be C_s. The mineral glaucosphaerite is equally enigmatic and may be monoclinic. Williams reported the structure of the rosasite group of minerals to be triclinic [1]. It is not neccessarily true that rosasite has the same structure as malachite [1]. In the structure of rosasite some of the copper atoms in the model of malachite are replaced by zinc atoms.

The infrared spectra of selected minerals of the rosasite group in the OH stretching region are shown in Figure 4. Rosasite is characterised by two intense bands at 3401 and 3311 cm^{-1} with two additional bands at 3139 and 3486 cm^{-1}. The bands at 3486, 3401 and 3311 cm^{-1} are attributed to OH stretching vibrations whereas the bands at 3228 and 3139 cm^{-1} are ascribed to adsorbed water. If we use a Libowitzky type empirical formula [34] claculation of the hydrogen bond distances in the structure can be estimated. The bands at 3486, 3401, 3311 and 3139 cm^{-1} lead to hydrogen bond distances of 2.877, 2.80, 2.75 and 2.68 Å. The conclusion may be made that there are three different hydrogen bond distances of the OH units which are a weaker hydrogen bond strength than the hydrogen bond formed from adsorbed water. The mineral glaukosphaerite has infrared bands at 3529, 3402, 3309, 3191 and 3022 cm^{-1}. The bands at 3402 and 3309 cm^{-1} are in almost identical positions to those of rosasite. Because of the broad spectral profile in the OH stretching region variation in the bands at 3191 and 3022 cm^{-1} may occur. This makes the fitting of bands difficult. Similarly for the mineral kolwezite the two OH stretching vibrations are observed at 3401 and 3307 cm^{-1}. The infrared spectrum of mcguinnessite appears different. The two bands at 3407 and 3316 cm^{-1} are in common with the spectra of the other minerals. The other intense band at 3545 cm^{-1} may be due to an impurity. Powder X-ray diffraction shows that these minerals are not 100 % pure and are often mixed with other minerals of the rosasite group or related minerals.

The infrared spectra of selected rosasite minerals in the 900 to 1200 cm^{-1} region are shown in Figure 5. For rosasite two intense bands are observed at 1096 and 1046 cm^{-1}. The first band is assigned to the ν_1 symmetric stretching mode of the carbonate unit. Bands have been observed in the infrared spectra of malachite at 1095 cm^{-1} and 1090 cm^{-1} for azurite [4, 5]. The infrared spectrum of hydrocerrusite showed an intense band at 1090 cm^{-1} [35]. Interestingly the $(CO_3)^{2-}$ ν_1 band of the rosasite minerals should not be infrared active [5, 36-38]. However because of symmetry reduction of the carbonate anion the band is activated. An intense Raman band is observed at 1096 cm^{-1} for rosasite and is assigned to the ν_1 $(CO_3)^{2-}$ symmetric stretching vibration [5, 36-38]. The intense band at 1046 cm^{-1} is assigned to the δ OH deformation mode. For malachite two bands attributed to OH deformation modes are found at 1045 and 875 cm^{-1} [5]. For hydrocerrusite the OH deformation modes were observed at 1047 and 1040 cm^{-1}. It is noted that in the infrared spectrum of rosasite an intense shoulder occurs at 1023 cm^{-1}. This band is also assigned to an OH

deformation mode [39, 40]. In the Raman spectrum of rosasite a low intensity band is observed at 1056 cm^{-1} and is ascribed to this vibrational mode [5, 36, 38, 41].

For the mineral kolwezite two intense infrared bands are observed at 1096 and 1047 cm^{-1}. The first band is assigned to the ν_1 $(CO_3)^{2-}$ vibrational mode and the second band to a δ OH deformation mode. As for rosasite in the infrared spectrum a long tail on the low wavenumber side is observed and a component band may be resolved at 1012 cm^{-1}. This band is a second δ OH deformation mode. The position of this second band appears to vary between the rosasite minerals. In the IR spectrum of mcguinnessite, two bands are observed at 1046 and 1004 cm^{-1}. Both bands are ascribed to δ OH deformation modes. The ν_1 $(CO_3)^{2-}$ symmetric stretching mode is observed at 1099 cm^{-1}. A second band is observed at 1084 cm^{-1}. The observation of a second band supports the concept of two different carbonate units in the mcguinnessite structure. In the Raman spectrum the intensity of bands assigned to δ OH deformation modes is low and for mcguinnessite a band is observed at 1060 cm^{-1}. In the infrared spectrum of glaukosphaerite the δ OH deformation mode is observed at 1047 cm^{-1}. However the spectral profile on the lower wavenumber side of this band is complex and may be resolved into a series of overlapping bands. Two bands are observed at 1099 and 1078 cm^{-1} and are assigned to the ν_1 symmetric stretching modes; again supporting the concept of two different carbonate units in the glaukosphaerite structure. Only a single ν_1 symmetric stretching mode band for rosasite was observed.

The infrared spectra of selected rosasite minerals in the 1225 to 1625 cm^{-1} region are shown in Figure 6. The infrared spectrum of rosasite in this spectral region are characterised by strong bands centred upon 1488 and 1388 cm^{-1} which may be resolved into four bands at 1522, 1488, 1425 and 1388 cm^{-1}. These bands are attributed to the ν_3 antisymmetric $(CO_3)^{2-}$ stretching modes. In the IR spectrum of malachite two bands are observed at around 1500 and 1400 cm^{-1} [5]. For hydrozincite two bands are observed at 1515 and 1400 cm^{-1}. It would appear that there are two pairs of bands for rosasite namely (1522 and 1425 cm^{-1}) and (1488 and 1388 cm^{-1}). The observation of two sets of bands for rosasite suggests that there are two independent carbonate units in the crystal structure. Such sets of bands are also observed for each of the other rosasite minerals. For kolwezite two sets of bands are found at (1522 and 1426 cm^{-1}) and (1486 and 1390 cm^{-1}) and for glaukosphaerite (1531 and 1425 cm^{-1}) and (1493 and 1401 cm^{-1}). The intensities for mcguinnessite are opposite to that of rosasite in this spectral region; bands are observed for this mineral at (1542 and 1432 cm^{-1}) and (1497 and 1391 cm^{-1}).

The infrared spectrum of the low wavenumber region are shown in Figure 7. The infrared spectrum is limited to the cut-off point at 550 cm^{-1} at which point the diamond ATR cell absorbs the infrared radiation. However such a cut off point does not effect the infrared spectroscopy of minerals containing carbonate as all of the bands are above 550 cm^{-1}. The mineral rosasite shows two intense infrared bands at 870 and 818 cm^{-1}. These bands are assigned to the ν_2 bending modes of the $(CO_3)^{2-}$ units. The observation of two ν_2 bands is in harmony with the observation of two sets of bands in the ν_3 antisymmetric stretching region. The infrared spectrum of malachite shows two bands at 820 and 803 cm^{-1} ascribed to ν_2 bending modes as does azurite at 837 and 817 cm^{-1}[5]. Hydrocerrusite infrared spectrum shows two bands at 850 and 834 cm^{-1}. The ~880 cm^{-1} band for rosasite is not symmetrical and may be

resolved into two component bands at 889 and 870 cm^{-1}. The infrared spectrum of the mineral glaucosphaerite is very similar to that of rosasite with two bands observed at 886 and 819 cm^{-1}. The infrared spectrum of the mineral kolwezite is also similar in this spectral region, even though the profile is more complex. The spectrum of mcguinnessite is more complex with a number of bands observed at 870, 847, 833, 819 and 803 cm^{-1}. The bands at 870 and 819 cm^{-1} are related to the ν_2 bending modes. The other bands may be due to impurities.

For rosasite a number of bands are observed at 781, 748 and 710 cm^{-1}. These bands are assigned to the ν_4 $(CO_3)^{2-}$ bending modes. For malachite two infrared bands are observed at 748 and 710 cm^{-1} which are assigned to this vibration [4, 5]. Another mineral with similar formulation to rosasite, hydrozicite has bands in this region at 738 and 710 cm^{-1}. The infrared spectrum of hydrocerrusite has ν_4 $(CO_3)^{2-}$ bending modes at 700, 687 and 676 cm^{-1}. Two bands are observed around 570 cm^{-1} for rosasite; it is not known if these bands are due to ν_4 $(CO_3)^{2-}$ bending modes. However this asignment seems unlikely. These bands are due to CuO stretching vibrations [41-45]. The infrared spectrum of kolwezite displays bands at 747, 728 and 710 cm^{-1}. The results for glaukosphaerite include bands at 749, 737 and 668 cm^{-1}. A low intensity band is observed at 570 cm^{-1} and is ascribed to the CuO stretching vibration. The IR spectrum of mcguinnessite also shows an intense band at 559 cm^{-1} which is assigned to CuO stretching vibration [42, 45-47].

CONCLUSIONS

XRD studies of the rosasite mineral group showed the minerals are mixtures of members of the rosasite minerals. Normally one of the rosasite minerals is predominant. EDAX has been used to determine the chemical composition of the mineral. The rosasite from Rosas mine, Narcao, Cagliari, Sardegna (Sardinia), Italy analysed as CuO 53.7 and ZnO 18.3 % giving rise to the formula $(Cu_{1.5}Zn_{0.5})_2(CO)_3(OH)_2$. Glaucosphaerite from the Carr Boyd Nickel mine analysed as CuO 41.6 % and NiO 25.2 % giving rise to the formula $(Cu_{1.1}Ni_{0.7}Mg_{0.06})_2(CO)_3(OH)_2$. Similarly the mineral kolwezite from Zairehas a formula $(Cu_{1.33}Co_{0.67})_2(CO)_3(OH)_2$.

The infrared spectral patterns for the minerals rosasite, glaucosphaerite, kolwezite and mcguinnessite are similar and may be compared with that of malachite. This implies the molecular structure is similar to malachite. The single crystal structure of the members of the rosasite mineral group remains undetermined. The question arsies as to why there are similar infrared spectral patterns for the rosasite minerals. It means the minerals must have the same structure or at least related structures. Malachite is monoclinic with point group 2/*m*. Therefore it can be inferred that the structure of the rosasite group of minerals is monoclinic. This conclusion is in agreement with the assumptions of Anthony et al. who state that rosasite and related minerals have monoclinic structure by analogy with malachite [33].

Acknowledgments

The financial and infra-structure support of the Queensland University of Technology, Inorganic Materials Research Program is gratefully acknowledged. The Australian Research Council (ARC) is thanked for funding the instrumentation.

References

[1]. P. A. Williams, *Oxide Zone Geochemistry*, Ellis Horwood Ltd, Chichester, West Sussex, England, 1990.
[2]. J. A. Mandarino, *Fleischer's Glossary of Mineral Species*, The Mineralogical Record Inc., Tuscon, 1999.
[3]. J. L. Jambor, Paper - Geological Survey of Canada 76-1C (1976) 97.
[4]. R. L. Frost, Z. Ding, J. T. Kloprogge and W. N. Martens, Thermochim. Acta 390 (2002) 133.
[5]. R. L. Frost, W. N. Martens, L. Rintoul, E. Mahmutagic and J. T. Kloprogge, Journal of Raman Spectroscopy 33 (2002) 252.
[6]. D. Lovisato, Atti. accad. Lincei, [2] 17 (1910) 723.
[7]. G. P. Bolgov and N. A. Rozybakieva, Sbornik Nauch. Trudov Kazakh. Gorno-Met. Inst. (1956) 34.
[8]. C. Perrier, American Mineralogist 6 (1921) 166.
[9]. M. W. Pryce and J. Just, Mineralogical Magazine 39 (1974) 737.
[10]. L. B. Railsback, Carbonates and Evaporites 14 (1999) 1.
[11]. J. L. Jambor, Canadian Mineralogist 14, Pt. 4 (1976) 574.
[12]. M. Deliens and P. Piret, Bulletin de Mineralogie 103 (1980) 179.
[13]. A. J. Read, Mineralogical Magazine 48 (1984) 457.
[14]. W. Postl and P. Golob, Mitteilungsblatt - Abteilung fuer Mineralogie am Landesmuseum Joanneum 49 (1981) 293.
[15]. S. Matsubara and A. Kato, Ganko 88 (1993) 517.
[16]. R. C. Erd, F. P. Cesbron, F. E. Goff and J. R. Clark, Mineralogical Record 12 (1981) 143.
[17]. E. H. Nickel, J. A. Hallbert and R. Halligan, Journal of the Geological Society of Australia 26 (1979) 61.
[18]. E. H. Nickel and L. G. Berry, Canadian Mineralogist 19 (1981) 315.
[19]. E. H. Nickel, J. F. M. Clout and B. J. Gartrell, Mineralogical Record 25 (1994) 283.
[20]. F. Zigan, W. Joswig, H. D. Schuster and S. A. Mason, Zeitschrift fuer Kristallographie, Kristallgeometrie, Kristallphysik, Kristallchemie 145 (1977) 412.
[21]. J. A. Goldsmith and S. D. Ross, Spectrochimica Acta, Part A: Molecular and Biomolecular Spectroscopy 24 (1968) 2131.
[22]. C. Rodriguez P, Boletin de la Sociedad Quimica del Peru 35 (1969) 38.
[23]. K. Wada, Kanzei Chuo Bunsekishoho 19 (1978) 133.
[24]. P. Tarte, Proc. Intern. Meeting Mol. Spectry., 4th, Bologna, 1959 3 (1962) 1041.
[25]. P. Tarte and M. Deliens, Bulletin de la Societe Royale des Sciences de Liege 43 (1974) 96.
[26]. R. J. H. Clark, Journal of Molecular Structure 480-481 (1999) 15.
[27]. L. Burgio, D. A. Ciomartan and R. J. H. Clark, Journal of Raman Spectroscopy 28 (1997) 79.
[28]. M. Bouchard and D. C. Smith, Asian Chemistry Letters 5 (2001) 157.
[29]. B. Guineau, Studies in Conservation 29 (1984) 35.
[30]. C. Rocchiccioli, Compt. Rend. 259 (1964) 4581.
[31]. M. Schmidt and H. D. Lutz, Physics and Chemistry of Minerals 20 (1993) 27.
[32]. A. C. Roberts, J. L. Jambor and J. D. Grice, Powder Diffraction 1 (1986) 56.
[33]. J. W. Anthony, R. A. Bideaux, K. W. Bladh and M. C. Nichols, *Handbook of Mineralogy, Vol. 5*, Mineral Data Publishing, Tiscon, Arizona, USA, 2003.
[34]. E. Libowitzky, Monatshefte fuer Chemie 130 (1999) 1047.
[35]. R. L. Frost, W. Martens, J. T. Kloprogge and Z. Ding, Spectrochim. Acta, Part A 59A (2003) 2705.
[36]. R. L. Frost, P. A. Williams and W. Martens, Mineral. Mag. 67 (2003) 103.
[37]. R. L. Frost, D. A. Henry and K. Erickson, J. Raman Spectrosc. 35 (2004) 255.
[38]. R. L. Frost, K. L. Erickson, M. L. Weier, O. Carmody and J. Cejka, J. Mol. Struct. 737 (2005) 173.
[39]. W. N. Martens, L. Rintoul, J. T. Kloprogge and R. L. Frost, Am. Mineral. 89 (2004) 352.
[40]. B. J. Reddy and R. L. Frost, Neues Jahrb. Mineral., Monatsh. (2004) 525.
[41]. R. L. Frost and M. L. Weier, Thermochim. Acta 409 (2004) 79.
[42]. Z. Ding, R. L. Frost and J. T. Kloprogge, J. Mater. Sci. Lett. 21 (2002) 981.
[43]. R. L. Frost, Z. Ding, W. N. Martens and T. E. Johnson, Thermochim. Acta 398 (2003) 167.
[44]. R. L. Frost and M. L. Weier, Thermochim. Acta 406 (2003) 221.
[45]. R. L. Frost and Z. Ding, Thermochim. Acta 405 (2003) 207.
[46]. R. L. Frost, Z. Ding, W. N. Martens and T. E. Johnson, Thermochim. Acta 398 (2003) 167.

[47]. R. L. Frost, M. L. Weier, M. E. Clissold and P. A. Williams, Spectrochim. Acta, Part A 59 (2003) 3313.

Mineral	Locality of origin	Formulae	Analysis (% by mass)
Rosasite	Mapimi, Durango, Mexico	$(Cu,Zn)_2(CO)_3(OH)_2$	CuO 35.7 % ZnO 36.5 %
Glaukosphaerite	Carr Boyd Nickel Mine, Carr Boyd Rocks, W.A. [17, 19]	$(Cu,Ni)_2(CO_3)(OH)_2$	CuO 41.6 % NiO 25.2 %
Kolwezite	Mupine, Shaba Province, Zaire [33]	$(Cu,Co)_2(CO)_3(OH)_2$	CuO 48.4 % CoO 23.0 %
McGuinnessite	Red Mountain, Mendocino County, California [16]	$(Mg,Cu)_2(CO_3)(OH)_2$	CuO 39.6 % MgO 23.7%

Table 1 Table of the hydroxycarbonate minerals, their chemical formulae and origin

List of Figures

List of Tables

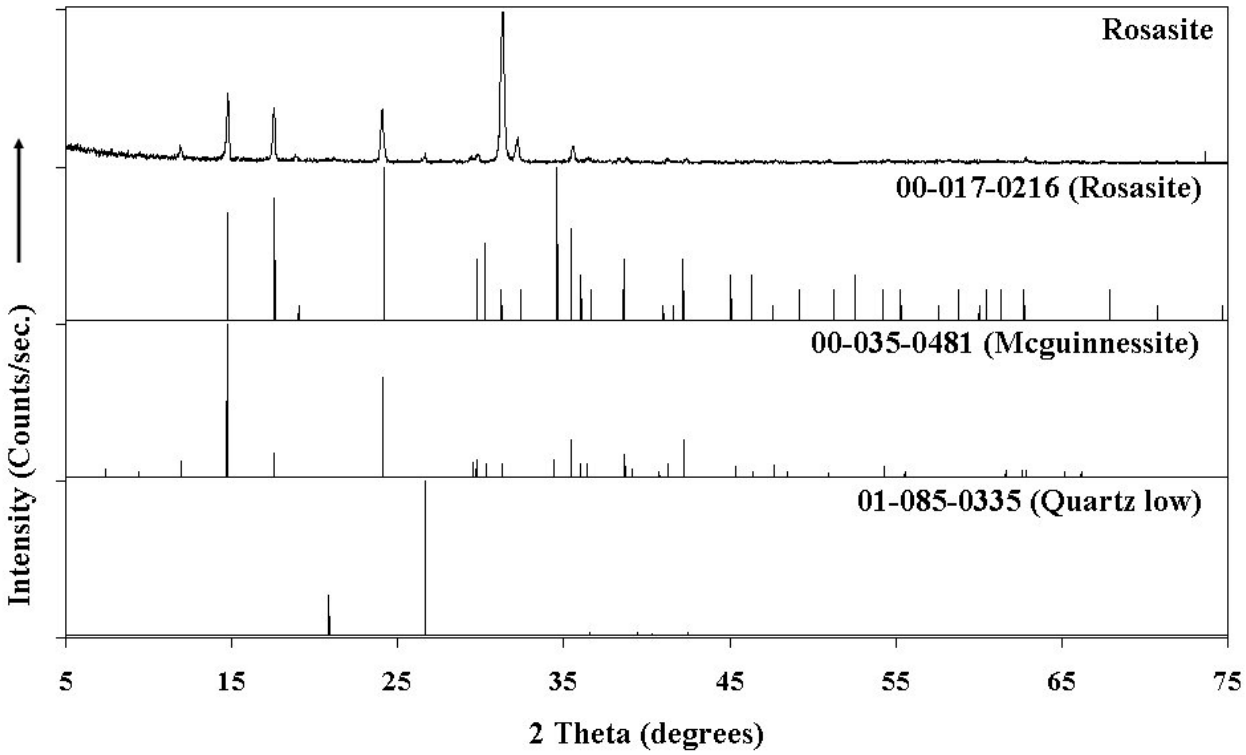
Rosasite
00-017-0216 (Rosasite)
00-035-0481 (Mcguinnessite)
01-085-0335 (Quartz low)
Intensity (Counts/sec.)
5
15
25
35
45
55
65
75
2 Theta (degrees)

Figure 1a

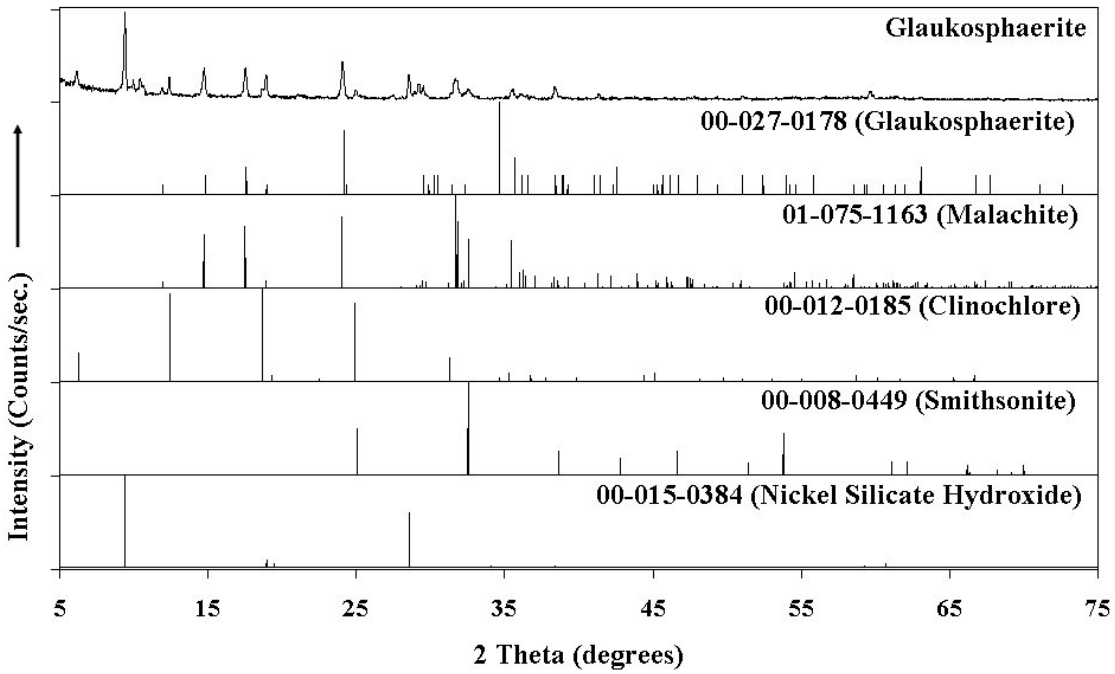
Glaukosphaerite
00-027-0178 (Glaukosphaerite)
01-075-1163 (Malachite)
00-012-0185 (Clinochlore)
00-008-0449 (Smithsonite)
00-015-0384 (Nickel Silicate Hydroxide)
Intensity (Counts/sec.)
5
15
25
35
45
55
65
75
2 Theta (degrees)

Figure 1b

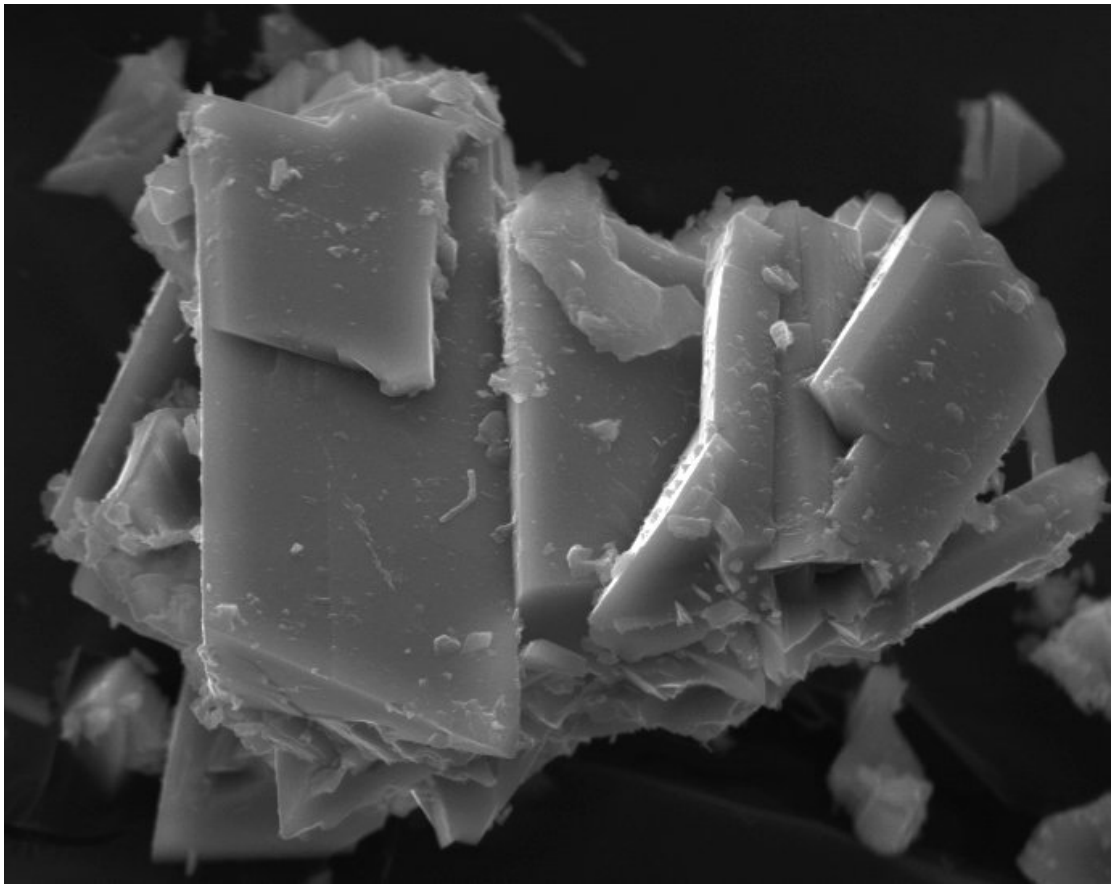

Figure 2a SEM image of rosasite

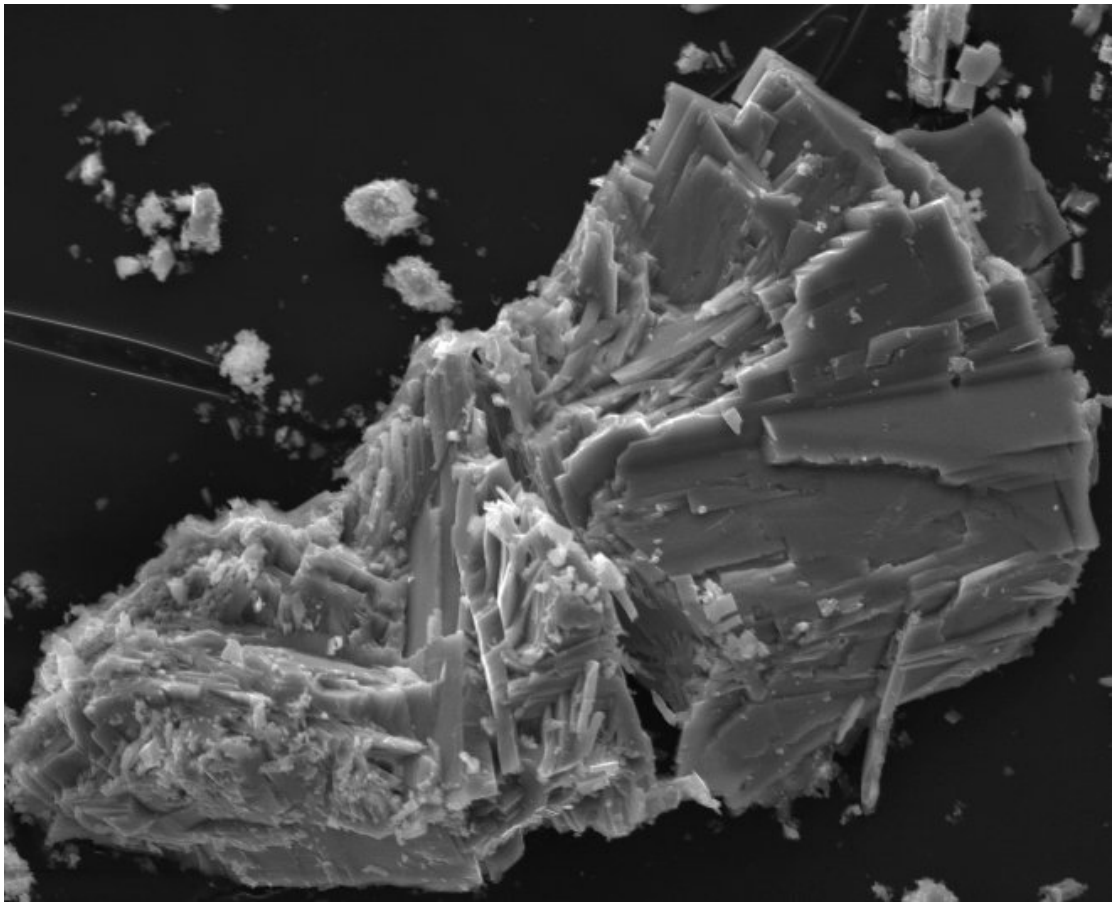

Figure 2b SEM image of glaukosphaerite

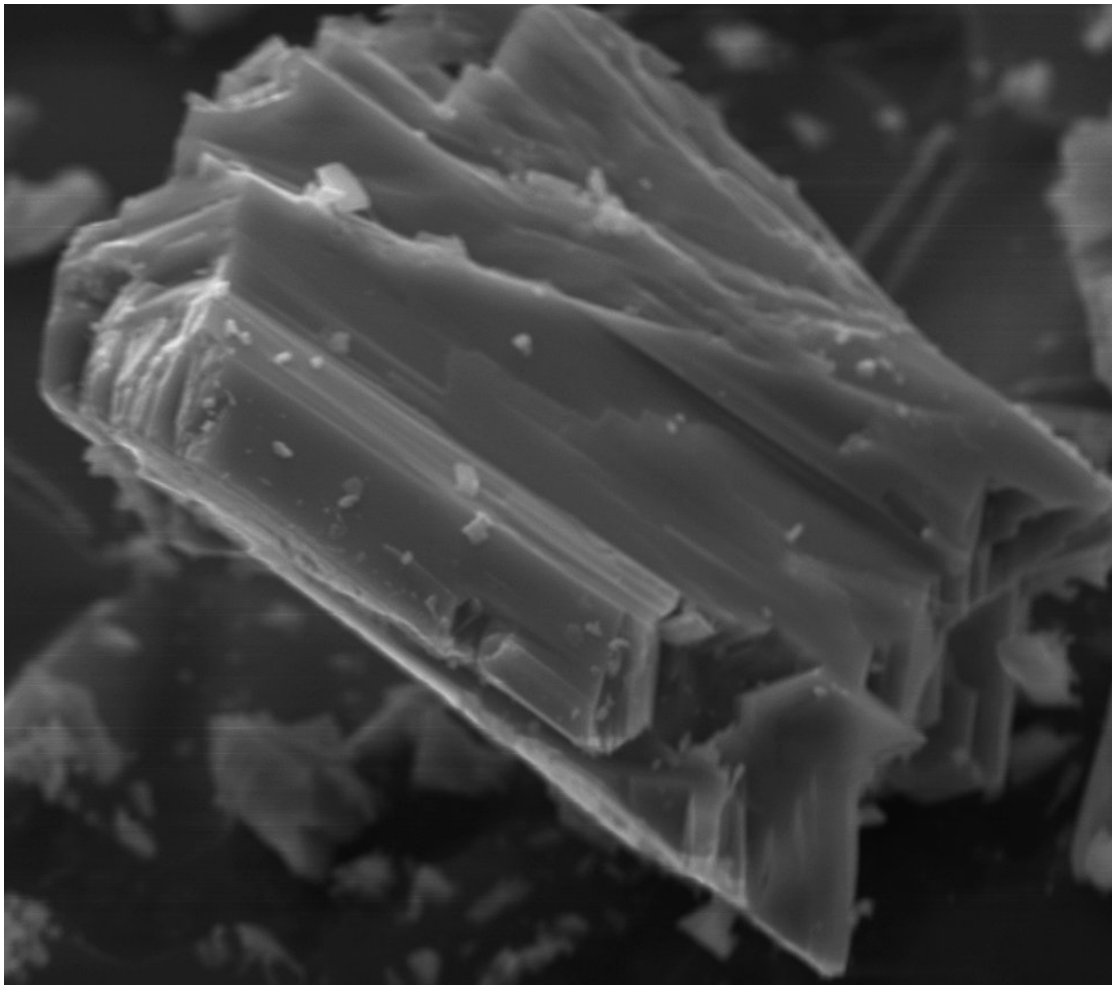

Figure 2c SEM image of kolwezite

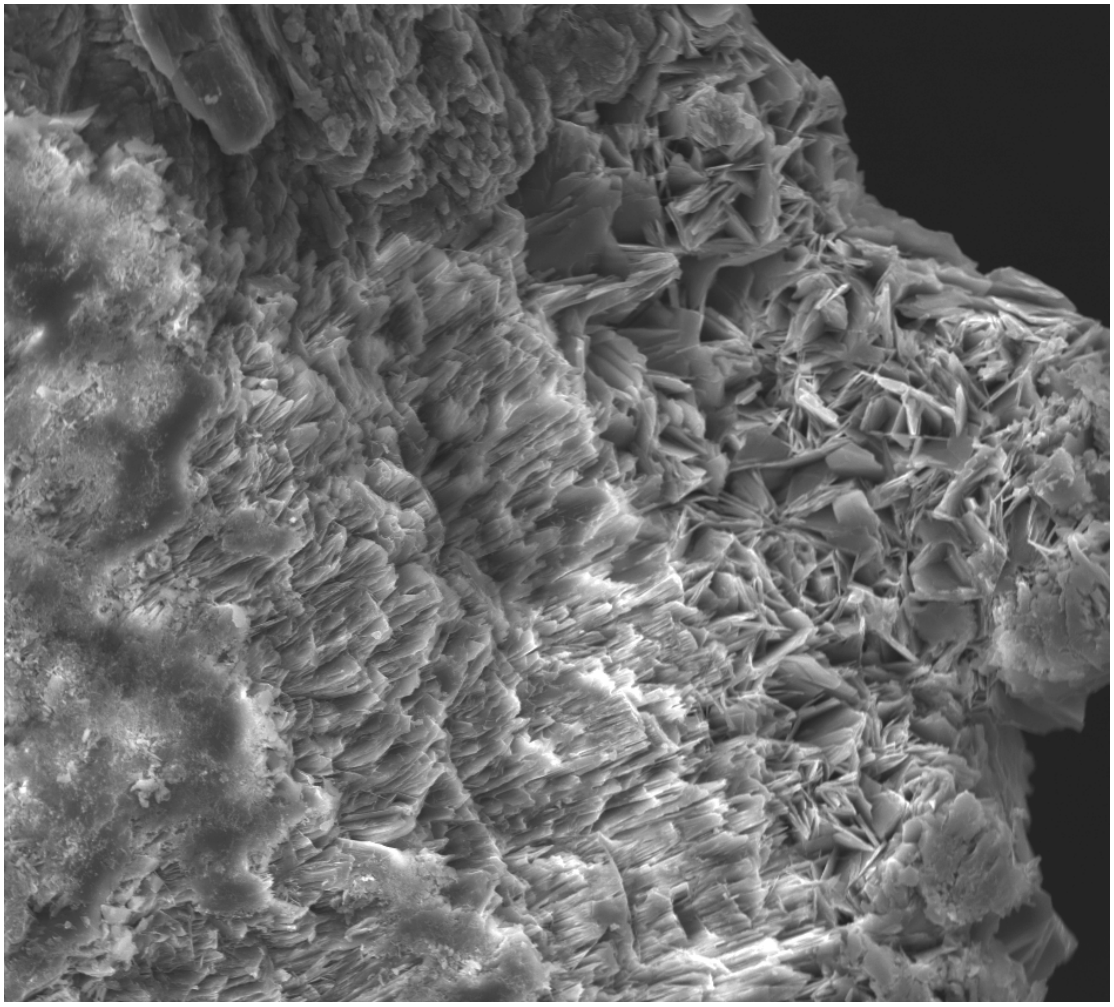

Figure 2d SEM image of pokrovskite

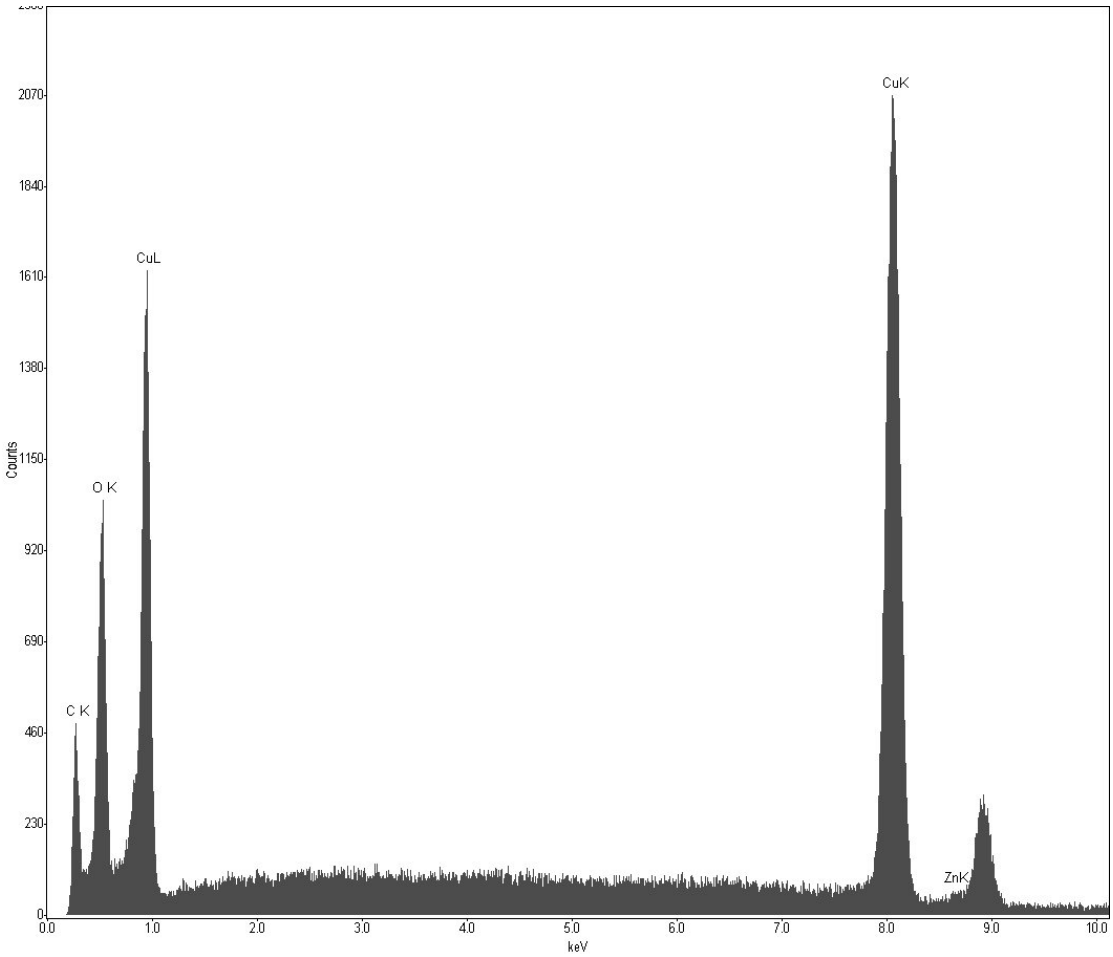

Figure 3a EDX of rosasite

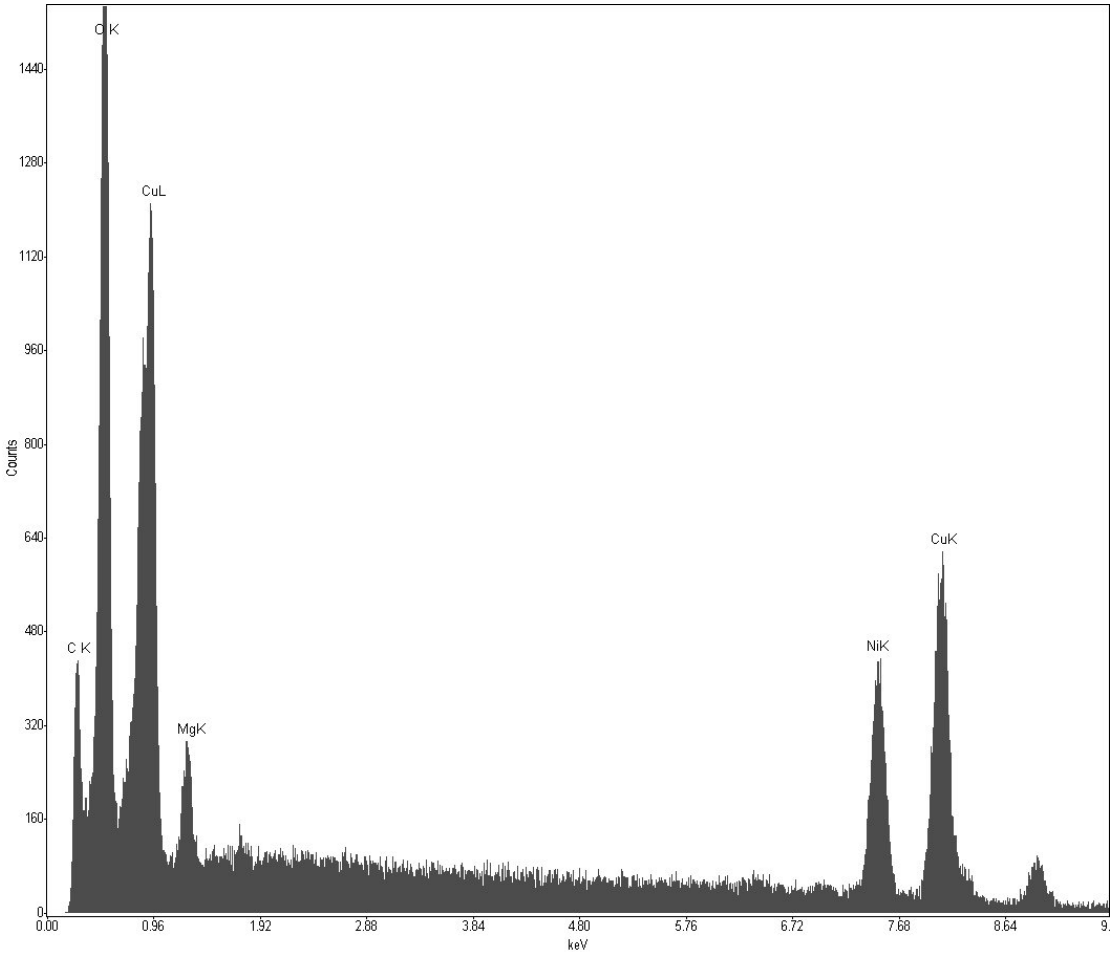

Figure 3b Glaucosphaerite

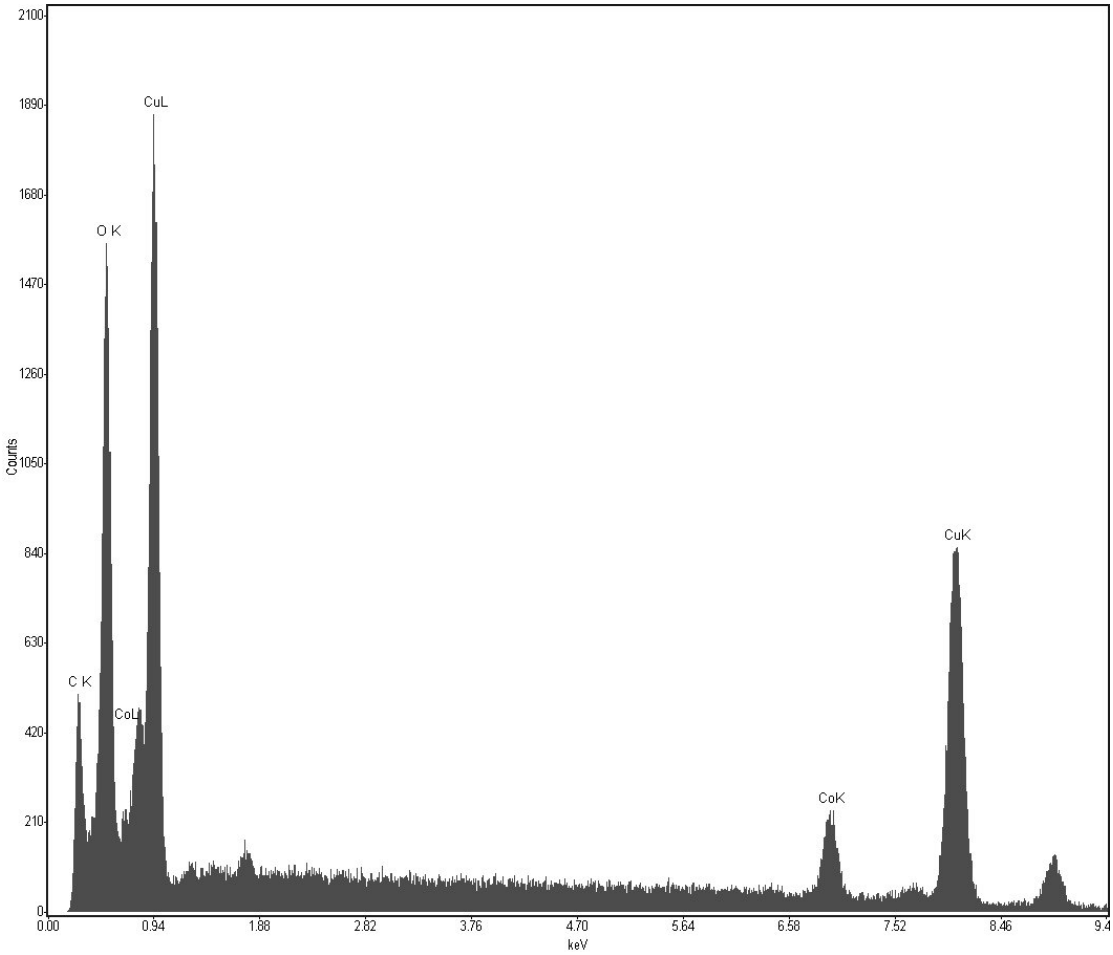

Figure 3c EDAX of kolwezite

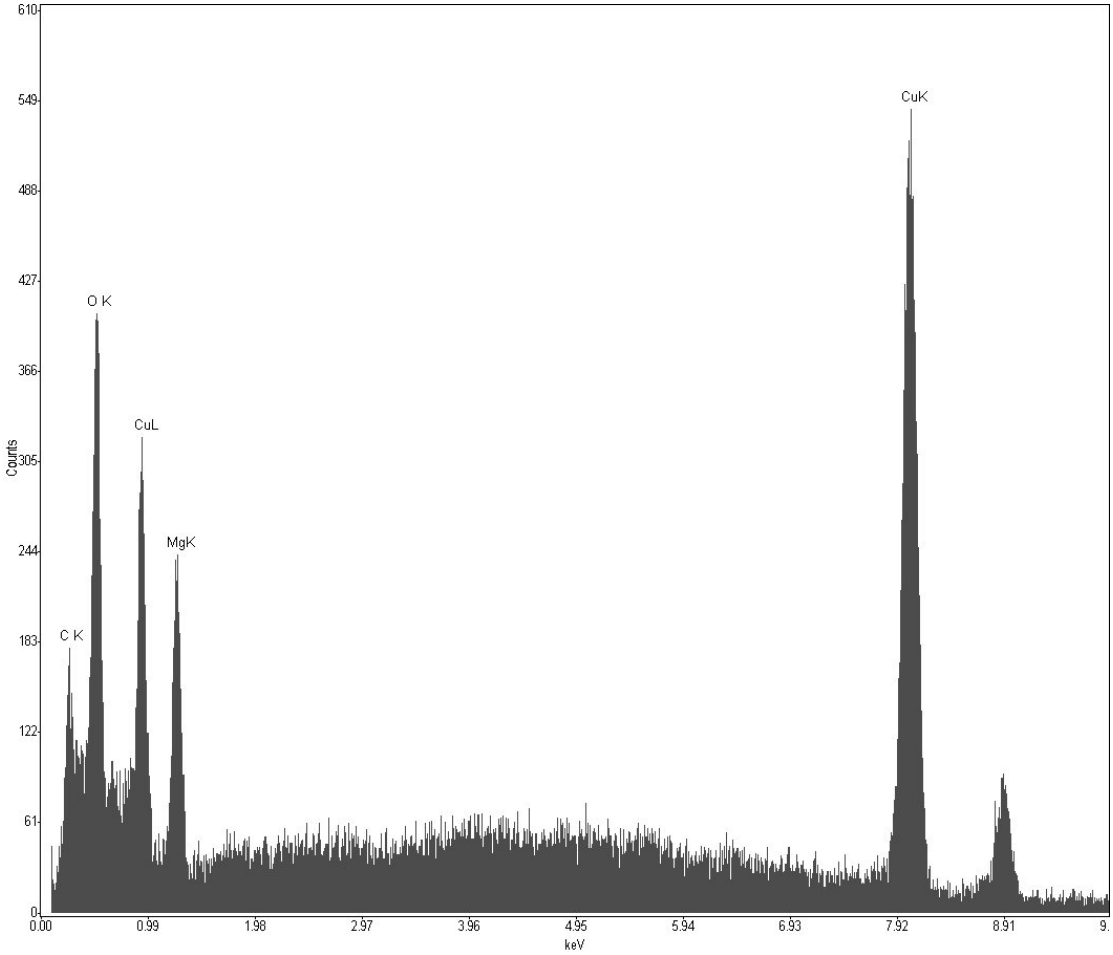

Figure 3d Mcguinnessite

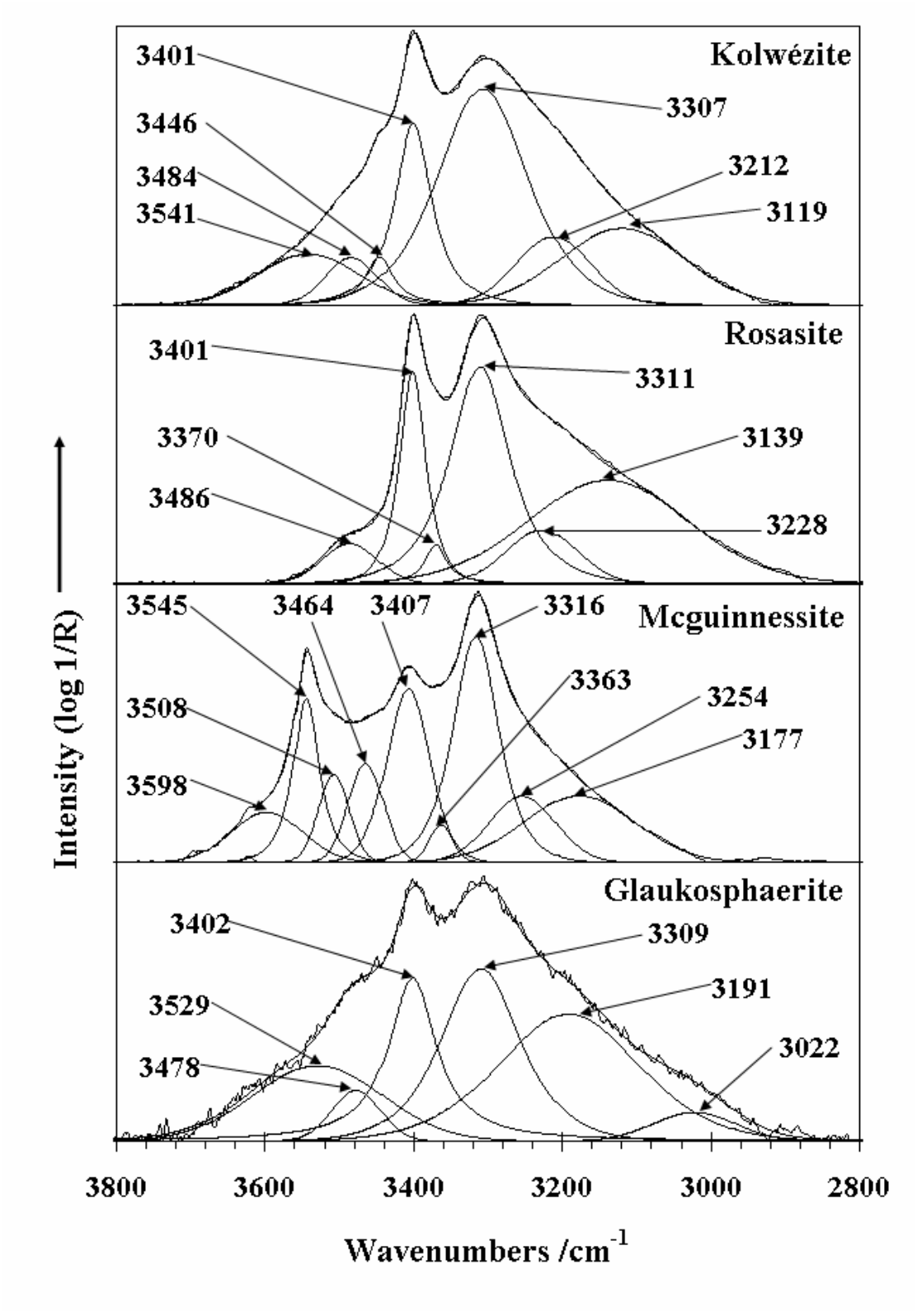
Kolwézite
3401
3307
3446
3212
3484
3119
3541
Rosasite
3401
3311
3370
3139
3486
3228
Mcguinnessite
3545
3464
3407
3316
3363
3508
3254
3177
3598
Glaukosphaerite
3402
3309
3191
3529
3022
3478
Intensity (log 1/R)
3800
3600
3400
3200
3000
2800
Wavenumbers /cm-1

Figure 4

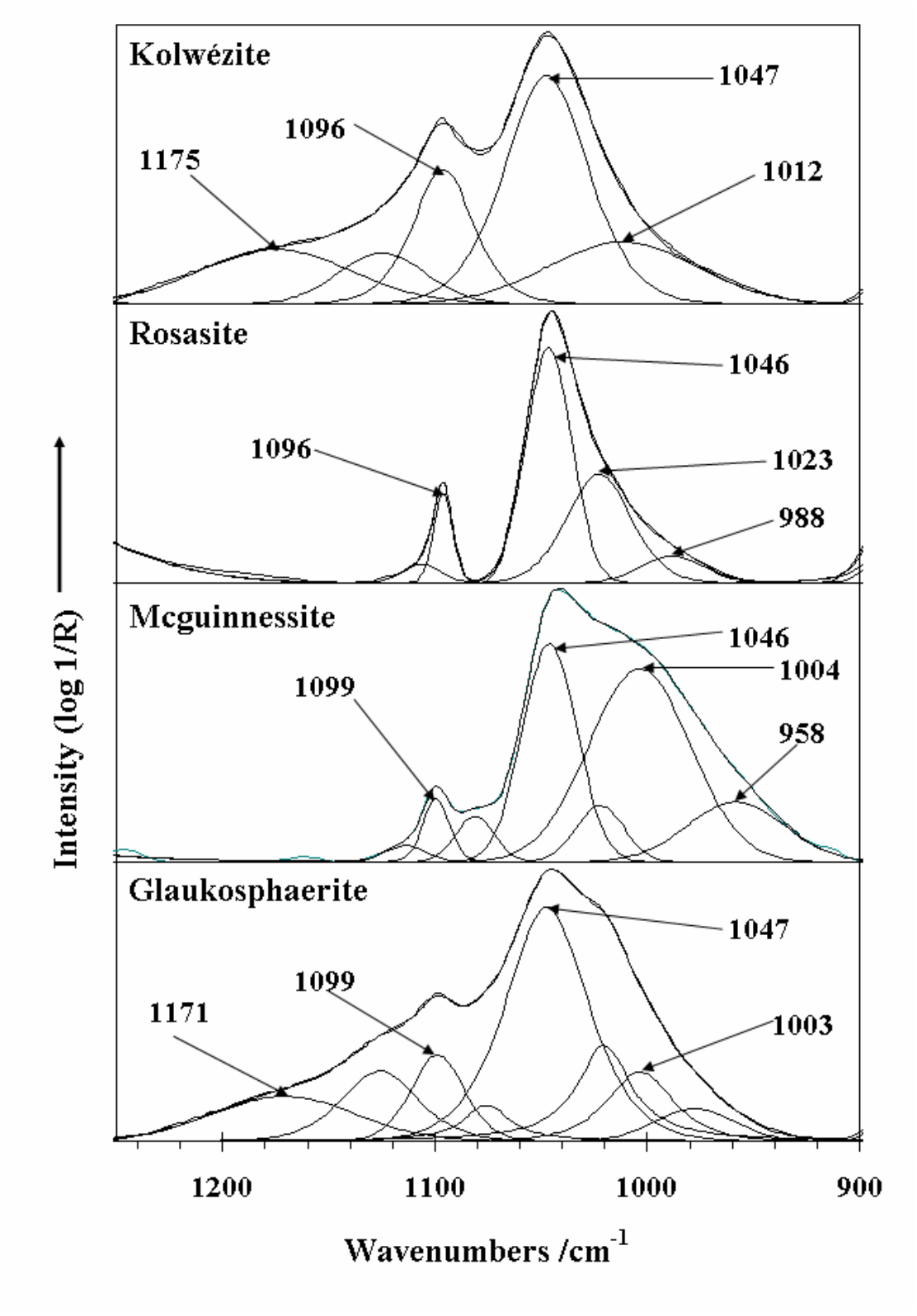
Kolwézite
1047
1096
1175
1012
Rosasite
1046
1096
1023
988
Mcguinnessite
1046
1004
1099
958
Glaukosphaerite
1047
1099
1171
1003
Intensity (log 1/R)
1200
1100
1000
900
Wavenumbers /cm-1

Figure 5

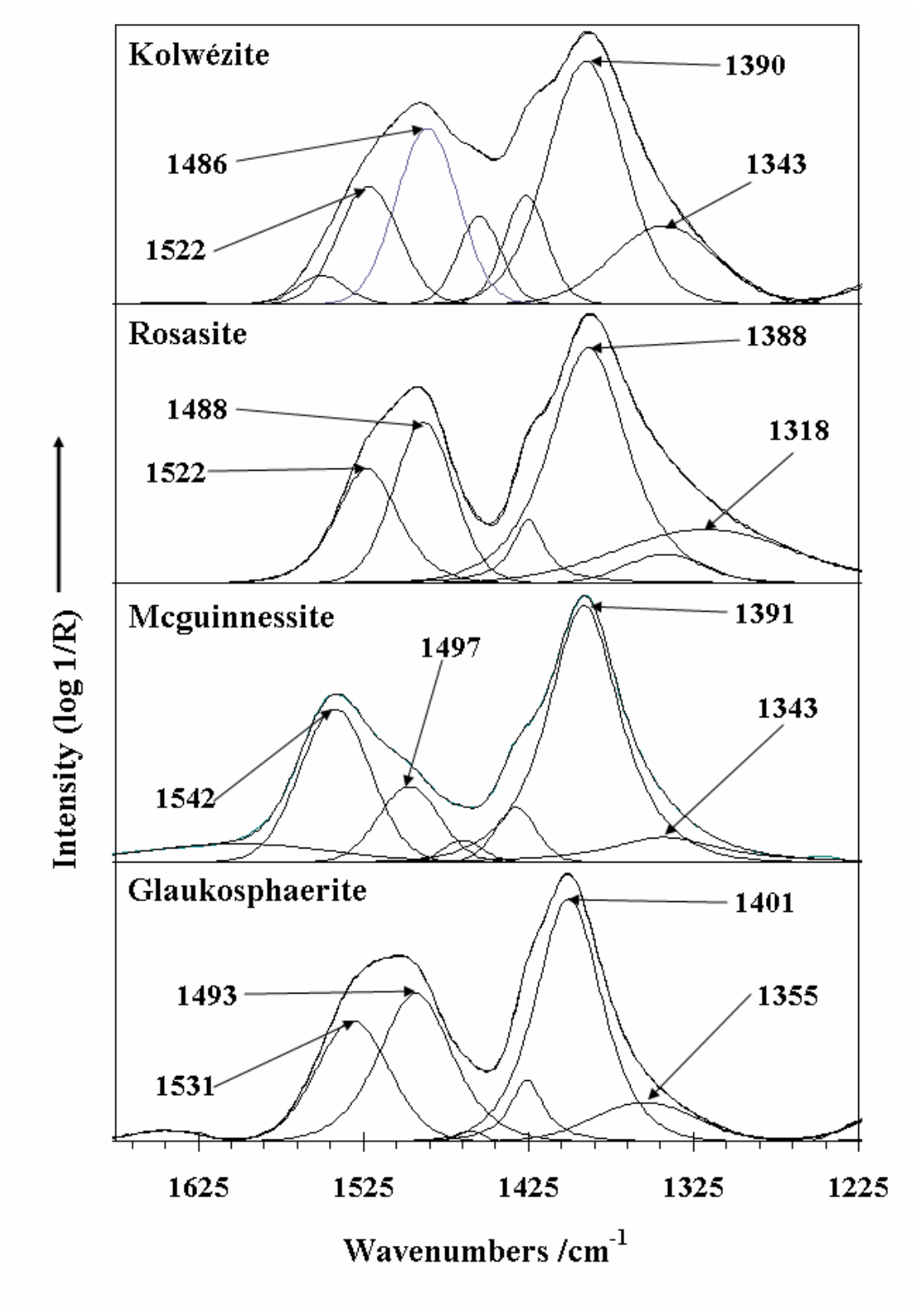
Kolwézite
1390
1486
1343
1522
Rosasite
1388
1488
1318
1522
Mcguinnessite
1391
1497
1343
1542
Glaukosphaerite
1401
1493
1355
1531
Intensity (log 1/R)
1625
1525
1425
1325
1225
Wavenumbers /cm-1

Figure 6

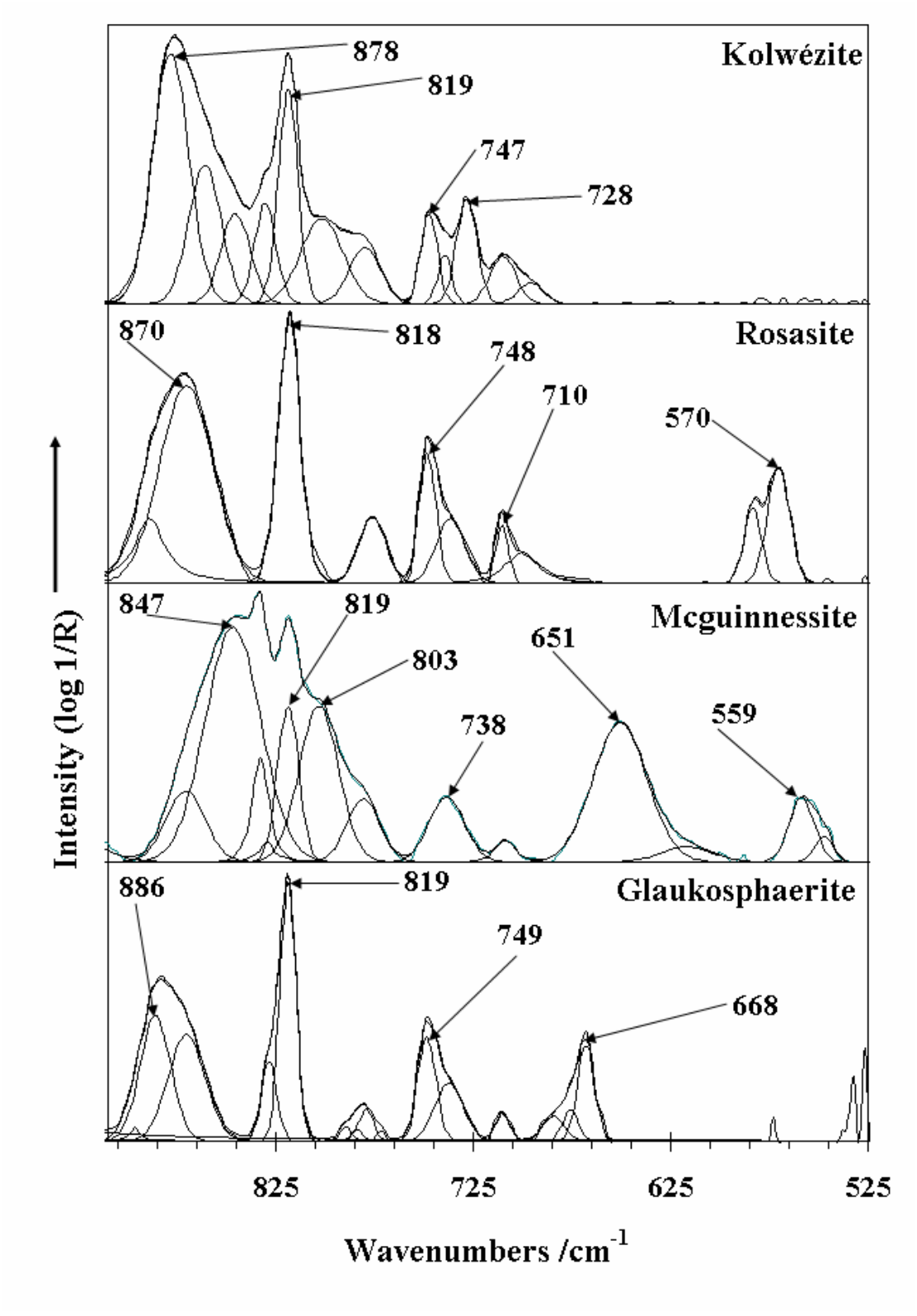
Kolwézite
878
819
747
728
Rosasite
870
818
748
710
570
Mcguinnessite
847
819
803
651
738
559
Glaukosphaerite
886
819
749
668
Intensity (log 1/R)
825
725
625
525
Wavenumbers /cm-1

Figure 7